Robust Transmission Waveform Design for Distributed Multiple-Radar Systems Based on Low Probability of Intercept

Chenguang Shi, Fei Wang, Mathini Sellathurai, Jianjiang Zhou, and Huan Zhang

This paper addresses the problem of robust waveform design for distributed multiple-radar systems (DMRSs) based on low probability of intercept (LPI), where signal-to-interference-plus-noise ratio (SINR) and mutual information (MI) are utilized as the metrics for target detection and information extraction, respectively. Recognizing that a precise characterization of a target spectrum is impossible to capture in practice, we consider that a target spectrum lies in an uncertainty class bounded by known upper and lower bounds. Based on this model, robust waveform design approaches for the DMRS are developed based on LPI-SINR and LPI-MI criteria, where the total transmitting energy is minimized for a given system performance. Numerical results show the effectiveness of the proposed approaches.

Keywords: Robust waveform design, distributed multiple-radar system, low probability of intercept, signal-to-interference-plus-noise ratio, mutual information, DMRS, LPI, SINR, MI.

I. Introduction

In recent years, research on distributed multiple-radar systems (DMRSs) has received increasing impetus. Compared to a traditional monostatic radar system, a DMRS can provide improved capabilities by employing waveform and spatial diversities [1]–[3].

Currently, some of the most important problems concerning DMRSs are that of transmission waveform design and optimization of target detection performance, which have been extensively studied from various perspectives [4]–[12].

It has been shown in some works that an optimized waveform can further enhance the performance of a DMRS. The author in [4] proposes a procedure to design an optimal waveform, which aims to maximize the signal-to-interference-plus-noise ratio (SINR) at the output of a multiple-input and multiple-output (MIMO) radar detector. In [5], Stoica and others investigate a probing-signal design for a co-located MIMO radar based on a transmit beam pattern to maximize the power around the locations of targets of interest. It is demonstrated that the performance of the MIMO radar can be remarkably improved with the proper choice of probing signals.

The application of information theory to radar systems was presented by Woodward more than fifty years ago [13], [14]. However, it is not until recently that Bell in [6] first applied mutual information (MI) to radar waveform design, through which he was able to demonstrate that an optimal information extraction solution is one whereby energy is distributed among target scattering modes. Lately, the MI criterion was introduced to MIMO radar waveform design and has been a long-term

research topic for many years. Yang and Blum in [7] develop a MIMO radar waveform design based on MI and minimum mean square error (MMSE), in which it is shown that the MI-based waveform design method is equivalent to the MMSE case. The work of [8] studies multi-static radar code design approaches using information-theoretic criteria in the presence of clutter, which can improve the detection performance significantly. In [9], a novel two-step strategy is proposed to design the waveforms of adaptive MIMO radar, where it is shown that the strategy can provide great performance enhancement in terms of target detection and feature extraction. Other existing studies [10]–[12] also exploit similar criteria to optimize radar waveforms.

Following from the above discussions, it is worth pointing out that most cases require only perfect knowledge of the target spectrum. However, one cannot obtain precise characteristics of a target spectrum in practice. Given such circumstances, robust methods seem quite attractive to tackle the aforementioned problems [15]. Some literatures utilize robust procedures for the purpose of waveform design in the presence of model uncertainties [16]–[18]. Moreover, up to now, we haven't seen any studies on robust radar waveform design for DMRSs based on low probability of intercept (LPI), which is playing an increasingly important role in electronic warfare [3]. This motivates us to address this matter.

This paper will investigate task-dependent robust transmission waveform design approaches based on LPI for DMRSs. The main contributions of this paper are summarized as follows. From a practical stand point, without a precise characterization of a target spectrum, we assume that the true target spectrum lies in an uncertainty class confined by known upper and lower bounds. Based on this band model, we develop robust waveform design approaches under both the LPI-SINR and the LPI-MI criteria. The proposed approaches bound the worst-case LPI performance in DMRSs. In particular, if the target spectrum lies in the uncertainty class, then the achievable LPI performance is always as good as or better than the robust waveforms in the worst case. Numerical results are provided to demonstrate that our proposed approaches optimize the worst-case LPI performance. No literature discussing LPI-based robust transmission waveform design methods for DMRSs existed prior to us conducting this work.

The rest of this paper is organized as follows. In Section II, we introduce a model for the detection of a signal of a known target, and also propose optimal waveform design methods based on LPI-SINR and LPI-MI given a precise characterization of a target spectrum. In Section III, by taking the uncertainty of the target spectrum into consideration, we investigate a robust waveform design based on both LPI-SINR

and LPI-MI, where the true target spectrum is presumed to lie within an uncertainty class bounded by known upper and lower bounds. A discussion of these two robust waveform design methods is also provided in this section. Numerical simulations are given in Section IV. Finally, conclusions are drawn in Section V.

II. Problem Formulation

1. Known-Target Signal Model in Signal-Dependent Interference

Figure 1 illustrates our model for the detection of a signal of a known target in signal-dependent interference, where $x_i(t)$ is the ith complex-valued baseband transmit waveform with finite duration T_i, and $h_i(t)$ is the ith known complex-valued baseband target impulse response of finite duration T_{h_i}. Let $X_i(f)$ and $H_i(f)$ denote the Fourier transforms of $x_i(t)$ and $h_i(t)$, respectively.

Let $\mathbf{n}_i(t)$ be the ith complex-valued zero-mean channel noise process with power spectral density (PSD) $S_i^n(f)$. Likewise, $\mathbf{c}_i(t)$ denotes the ith complex-valued, zero-mean Gaussian random process representing the signal-dependent interference with PSD $S_i^c(f)$. Further, $y_i(t)$ is the ith scattered signal, $r_i(t)$ is the ith complex-valued receiver filter impulse response, and $\mathbf{s}_{DMRS}(t)$ is the overall output signal. It is noted that the fusion center can process all the echoes reflected from the known target with the matched filter bank.

In this paper, we consider a scenario where all of a DMRS's radar nodes, individually and independently, detect the signal of a single known target. The nodes then proceeded to extract information about the signal. A phase code signal is utilized to resist any serious common-frequency interference among radar nodes [18]. It is also assumed that the DMRS has a precise knowledge of space and time. The information about the signal of the known target at each radar node is sent to a fusion center, which combines the local observations, $y_i(t)$, to improve the DMRS's system performance. A system model for the given
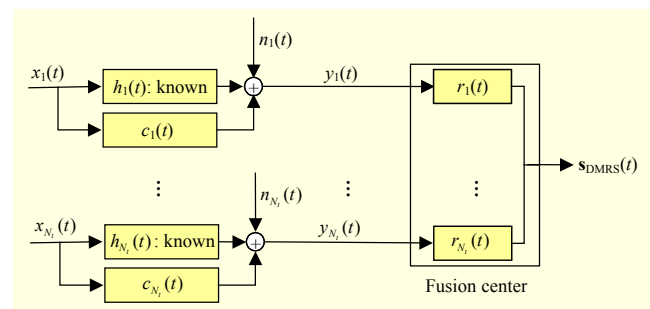

Fig. 1. Model for detection of signal of known target in signal-dependent interference.
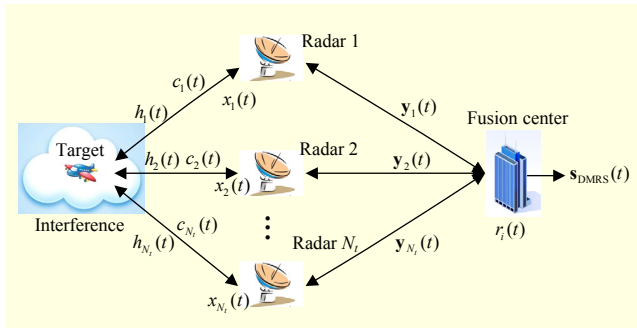
Fig. 2. System model for DMRS.

DMRS in the described scenario is depicted in Fig. 2. As illustrated in Fig. 2, the received signal, $s_{DMRS}(t)$, from the DMRS, is given by

$$
\begin{aligned}
s_{DMRS}(t) &= \sum_{i=1}^{N_t} s_i(t) \\
&= \sum_{i=1}^{N_t} r_i(t) * y_i(t) \\
&= \sum_{i=1}^{N_t} r_i(t) * \left[x_i(t) * h_i(t) + x_i(t) * c_i(t) + n_i(t) \right] \\
&= \sum_{i=1}^{N_t} r_i(t) * x_i(t) * h_i(t) + \sum_{i=1}^{N_t} r_i(t) * \left[x_i(t) * c_i(t) + n_i(t) \right] \\
&= s_s(t) + s_n(t),
\end{aligned}
$$

(1)

where $s_s(t)$ and $s_n(t)$ denote the signal and noise components of $s_{DMRS}(t)$, respectively.

2. Optimal Waveform Design Based on LPI-SINR

In this paper, the SINR is utilized as a metric for the target detection performance of the DMRS. We assume that the transmitting waveform signal is essentially limited by its own bandwidth (BW). With the derivation in [14], the overall SINR of the DMRS is written as

$$
\begin{aligned}
(SINR)_{DMRS} &\triangleq \sum_{i=1}^{N_t} SINR_i \\
&\simeq \sum_{i=1}^{N_t} \int_{BW} \frac{|H_i(f)|^2 \times |X_i(f)|^2 \times L_i^2}{S_i^c(f) \times |X_i(f)|^2 \times L_i^2 + S_i^n(f)} \, df,
\end{aligned}
$$

(2)

where L_i is the attenuation from the ith radar node of the DMRS to the known target; that is,

$$
L_i = \frac{\sqrt{G_{ti} \times G_{ri}}}{R_i^2},
$$

(3)

where G_{ti} is the gain of the ith radar's transmitting antenna, G_{ri} is the gain of the ith radar's receiving antenna, and R_i is the range from the ith radar node to the known target. In this case,

we can see that the SINR is related to the transmission waveforms, the target spectra, the noise PSD, and the interference PSD. Intuitively, maximization of SINR means better target detection performance for the DMRS. However, this also leads to the transmission of more energy by the DMRS, which means that the DMRS will ultimately become more vulnerable in modern electronic warfare.

Herein, we concentrate on an LPI-based optimal waveform design for the DMRS; the purpose of which is to minimize the total transmitting energy for a predefined threshold of SINR such that the LPI performance is met. An optimal waveform design based on LPI-SINR can be formulated as follows:

$$
\min_{|X_i(f)|^2, \forall i=1,\dots,N_t} \quad \sum_{i=1}^{N_t} \int_{BW} |X_i(f)|^2 \, df,
$$

$$
\text{s.t. } (SINR)_{DMRS} \simeq \sum_{i=1}^{N_t} \int_{BW} \frac{|H_i(f)|^2 \times |X_i(f)|^2 \times L_i^2}{S_i^c(f) \times |X_i(f)|^2 \times L_i^2 + S_i^n(f)} \, df \geq \gamma_{SINR}^{th},
$$

$$
\int_{BW} |X_i(f)|^2 \, df > 0 \qquad (\forall i),
$$

(4)

where γ_{SINR}^{th} denotes the predefined threshold of SINR in the DMRS.

Theorem 1. The optimal transmission waveforms that minimize the total transmitting energy, $\sum_{i=1}^{N_t} \int_{BW} |X_i(f)|^2 \, df$, under the SINR constraint, $(SINR)_{DMRS} \geq \gamma_{SINR}^{th}$, should satisfy

$$
|X_i(f)|^2 = \max\left[0, B_i(f)\left(A - D_i(f) \right) \right] \qquad (\forall i),
$$

(5)

where $B_i(f)$ and $D_i(f)$ can be given by

$$
B_i(f) = \frac{\sqrt{|H_i(f)|^2 \times S_i^n(f) \times L_i^2}}{S_i^c(f) \times L_i^2}
$$

(6)

and

$$
D_i(f) = \sqrt{\frac{S_i^n(f)}{|H_i(f)|^2 \times L_i^2}},
$$

(7)

respectively, and A is a constant determined by the SINR constraint

$$
\sum_{i=1}^{N_t} \int_{BW} \frac{|H_i(f)|^2 \times \max\left[0, B_i(f)\left(A - D_i(f) \right) \right] \times L_i^2}{S_i^c(f) \times \max\left[0, B_i(f)\left(A - D_i(f) \right) \right] \times L_i^2 + S_i^n(f)} \, df \geq \gamma_{SINR}^{th}.
$$

(8)

The solutions to (4) demonstrate that optimal transmission waveforms based on LPI-SINR for minimizing the total transmitting energy have frequency spectra obtained by performing a water-filling operation [12] on the functions $B_i(f)\left(A - D_i(f) \right) (\forall i)$. For a predefined threshold, γ_{SINR}^{th}, once A is obtained, $\sum_{i=1}^{N_t} \int_{BW} |X_i(f)|^2 \, df$ can be calculated by

substituting (5) into (4). The derivation of Theorem 1 is similar to [12].

3. Optimal Waveform Design Based on LPI-MI

As implied in [12], the MI between the DMRS echo and the target impulse response can be used as a metric for target estimation performance. The achievable MI in the DMRS is given by

$$(MI)_{DMRS} \triangleq \sum_{i=1}^{N_t} MI(y_i(t); h_i(t) \mid x_i(t))$$

$$\simeq \sum_{i=1}^{N_t} T_{y_i} \times \int_{BW} \ln \left\{ 1 + \frac{|H_i(f)|^2 \times |X_i(f)|^2 \times L_i^2}{T_{y_i} \times [S_i^c(f) \times |X_i(f)|^2 \times L_i^2 + S_i^n(f)]} \right\} df,$$

(9)

where $T_{y_i} = T_{h_i} + T_i (\forall i)$ denotes the duration of the echo $y_i(t)$. For brevity, we assume $T_y = T_{y_i} (\forall i)$, and (8) can be simplified as

$$(MI)_{DMRS} \simeq \sum_{i=1}^{N_t} T_y \times \int_{BW} \ln \left\{ 1 + \frac{|H_i(f)|^2 \times |X_i(f)|^2 \times L_i^2}{T_y \times [S_i^c(f) \times |X_i(f)|^2 \times L_i^2 + S_i^n(f)]} \right\} df.$$

(10)

From (10), one can observe that the MI is related to the transmitting waveforms, the target spectra, the noise PSD, and the interference PSD. It is indicated in [19] that maximizing MI between a DMRS return and a target impulse response can result in the DMRS having better capability to characterize the target, which also results in worse LPI performance. The optimal waveform design approach based on LPI-MI can be expressed as

$$\min_{|X_i(f)|^2, \forall i=1,\dots,N_t} \sum_{i=1}^{N_t} \int_{BW} |X_i(f)|^2 df,$$

$$\text{s.t. } (MI)_{DMRS} \simeq \sum_{i=1}^{N_t} T_y \times \int_{BW} \ln \left\{ 1 + \frac{|H_i(f)|^2 \times |X_i(f)|^2 \times L_i^2}{T_y \times [S_i^c(f) \times |X_i(f)|^2 \times L_i^2 + S_i^n(f)]} \right\} df \geq \gamma_{MI}^{th},$$

$$\int_{BW} |X_i(f)|^2 df > 0 \qquad (\forall i),$$

(11)

where γ_{MI}^{th} denotes the predetermined threshold of MI in the DMRS.

Theorem 2. The optimal transmission waveforms that minimize the total transmitting energy $\sum_{i=1}^{N_t} \int_{BW} |X_i(f)|^2 df$ under the MI constraint $(MI)_{RSN} \geq \gamma_{MI}^{th}$ should satisfy

$$|X_i(f)|^2 \simeq \max[0, B_i(f)(A - D_i(f))] \qquad (\forall i), \quad (12)$$

where $B_i(f)$ and $D_i(f)$ can be given by

$$B_i(f) = \frac{|H_i(f)|^2 \times L_i^2 / T_y}{2 S_i^c(f) \times L_i^2 + |H_i(f)|^2 \times L_i^2 / T_y} \qquad (13)$$

and

$$D_i(f) = \frac{S_i^n(f)}{|H_i(f)|^2 \times L_i^2 / T_y}, \qquad (14)$$

respectively, and A is a constant calculated by the MI constraint

$$\sum_{i=1}^{N_t} T_y \times \int_{BW} \ln \left\{ 1 + \frac{|H_i(f)|^2 \times \max[0, B_i(f)(A - D_i(f))] \times L_i^2}{T_y \times [S_i^c(f) \times \max[0, B_i(f)(A - D_i(f))] \times L_i^2 + S_i^n(f)]} \right\} df \geq \gamma_{MI}^{th}.$$

(15)

The LPI-MI-based optimal transmission waveforms also perform water-filling operations, and A controls the transmitting energy. The approximate transmitting energy $\sum_{i=1}^{N_t} \int_{BW} |X_i(f)|^2 df$ can then be calculated by substituting (12) into (11). The derivation of Theorem 2 is similar to [12].

III. Robust Transmission Waveform Design

In this section, we consider the uncertainty of the target spectrum, where a precise characterization of it is unknown because the exact target-radar orientation (TRO) is practically imprecise. The target spectrum in the direction of radar node $i (\forall i = 1,\dots,N_t)$ is assumed to be in a set, called an uncertainty class $(\aleph_i)$, bounded by known upper and lower bounds. As shown in Fig. 3, the nominal target spectrum is illustrated by the blue solid line, and the upper and lower bounds of the uncertainty class at each frequency are depicted by the error bars; that is, the nominal value plus or minus a random number between zero and one. The samples of the target spectrum in the direction of radar node i satisfy

$$\aleph_i = \{0 \leq l_{i,k} \leq H_i(f_k) \leq u_{i,k}, \ \forall k = 1,\dots,K\} \quad (\forall i), \quad (16)$$

where $\{f_k\}$ are the frequency samples. Let $u_{i,k}$ denote the upper bound at frequency f_k of radar node i. Likewise, $l_{i,k}$ denotes the lower bound at frequency f_k of radar node i. Furthermore, since a confidence band for the target spectrum could be determined via spectrum estimation, this band model is widely used in robust signal processing. It is reasonable to obtain the upper and lower bounds for the estimated target spectrum by field measurement and modeling [16]. It is worth noting that a larger difference between the upper and lower bounds indicates greater uncertainty about the known target. In addition, we should note that the distance between the upper and lower bounds at each frequency might be different.

Based on the band model, the robust transmission waveform $X_i^{robust}(f)$ is the optimal waveform for the worst case, $H_i(f) = H_i^{worst}(f)$, where $H_i^{worst}(f)$ is referred to as the least favorable target spectrum. If other waveforms are utilized, then the achievable LPI performance of the DMRS will be
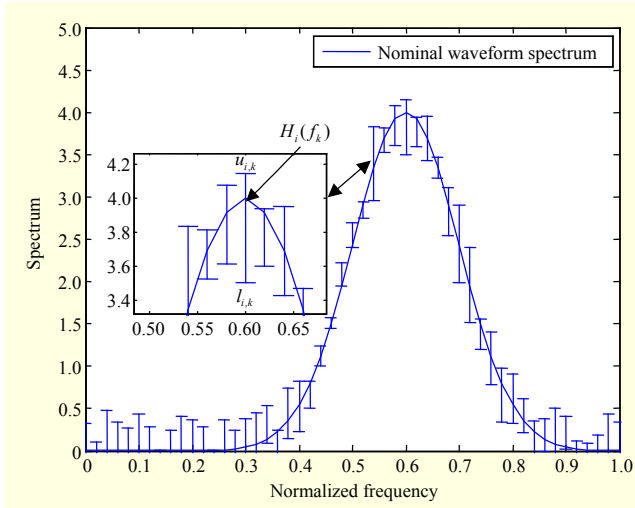
Fig. 3. Illustration of bounded target spectrum.

degraded; whereas, if the robust transmission waveform $X_i^{\text{robust}}(f)$ is employed, then the LPI performance will be always as good as or better than the case $H_i(f) = H_i^{\text{worst}}(f)$ for all the target spectra in the uncertainty class, which means that the achievable LPI performance will never be worse than this limit. Thus, the robust transmission waveform is optimum for the worst-case target spectrum in the uncertainty class. We can conclude that employing a robust transmission waveform design is a well-accepted engineering approach.

1. Robust Waveform Design Based on LPI-SINR

As suggested by the robust signal processing methodology described in [15], it is noted that it would be wise to use the robust waveform design approach to guarantee the worst-case LPI performance of the DMRS. Therefore, the robust waveform design approach based on LPI-SINR can be written as

$$\min_{|X_i(f)|^2, \forall i=1,\ldots,N_t} \sum_{i=1}^{N_t} \int_{\text{BW}} |X_i(f)|^2 \, df,$$

$$\text{s.t. (SINR)}_{\text{DMRS}} \simeq \sum_{i=1}^{N_t} \int_{\text{BW}} \frac{|H_i(f)|^2 \times |X_i(f)|^2 \times L_i^2}{S_i^{\text{c}}(f) \times |X_i(f)|^2 \times L_i^2 + S_i^{\text{n}}(f)} \, df \Bigg|_{|H_i(f)| \in \aleph_i} \geq \gamma_{\text{SINR}}^{\text{th}},$$

$$\int_{\text{BW}} |X_i(f)|^2 \, df > 0 \qquad (\forall i),$$

(17)

which is equivalent to the following problem:

$$\min_{|X_i(f)|^2, \forall i=1,\ldots,N_t} \sum_{i=1}^{N_t} \int_{\text{BW}} |X_i(f)|^2 \, df,$$

$$\text{s.t. (SINR)}_{\text{DMRS}} \simeq \sum_{i=1}^{N_t} \int_{\text{BW}} \frac{|L_i(f)|^2 \times |X_i(f)|^2 \times L_i^2}{S_i^{\text{c}}(f) \times |X_i(f)|^2 \times L_i^2 + S_i^{\text{n}}(f)} \, df \geq \gamma_{\text{SINR}}^{\text{th}},$$

$$\int_{\text{BW}} |X_i(f)|^2 \, df > 0 \qquad (\forall i),$$

(18)

where $|L_i(f)| = \{l_{i,k}, k=1,\ldots,K\}$ $(\forall i=1,\ldots,N_t)$ denotes the lower bound of the target spectrum uncertainty class in the direction of radar i.

Theorem 3. The robust optimal transmission waveforms for the model for the detection of a signal of a known target, which optimize (18), can be found by

$$\left|X_i^{\text{robust}}(f)\right|^2 = \max\left[0, \overline{B}_i(f)\left(\overline{A} - \overline{D}_i(f)\right)\right] \qquad (\forall i), \quad (19)$$

where $\overline{B}_i(f)$ and $\overline{D}_i(f)$ can be given by

$$\overline{B}_i(f) = \frac{\sqrt{|L_i(f)|^2 \times S_i^{\text{n}}(f)} \times L_i^2}{S_i^{\text{c}}(f) \times L_i^2} \qquad (20)$$

and

$$\overline{D}_i(f) = \sqrt{\frac{S_i^{\text{n}}(f)}{|L_i(f)|^2 \times L_i^2}}, \qquad (21)$$

respectively, and the constant $\overline{A}$ is chosen to satisfy

$$\sum_{i=1}^{N_t} \int_{\text{BW}} \frac{|L_i(f)|^2 \times \max\left[0, \overline{B}_i(f)\left(\overline{A} - \overline{D}_i(f)\right)\right] \times L_i^2}{S_i^{\text{c}}(f) \times \max\left[0, \overline{B}_i(f)\left(\overline{A} - \overline{D}_i(f)\right)\right] \times L_i^2 + S_i^{\text{n}}(f)} \, df \geq \gamma_{\text{SINR}}^{\text{th}}.$$

(22)

2. Robust Waveform Design Based on LPI-MI

The robust waveform design approach based on LPI-MI aims to solve

$$\min_{|X_i(f)|^2, \forall i=1,\ldots,N_t} \sum_{i=1}^{N_t} \int_{\text{BW}} |X_i(f)|^2 \, df,$$

$$\text{s.t. (MI)}_{\text{DMRS}} \simeq \sum_{i=1}^{N_t} T_y \times \int_{\text{BW}} \ln\left\{1 + \frac{|H_i(f)|^2 \times |X_i(f)|^2 \times L_i^2}{T_y \times \left[S_i^{\text{c}}(f) \times |X_i(f)|^2 \times L_i^2 + S_i^{\text{n}}(f)\right]}\right\} df \Bigg|_{|H_i(f)| \in \aleph_i} \geq \gamma_{\text{MI}}^{\text{th}},$$

$$\int_{\text{BW}} |X_i(f)|^2 \, df > 0 \qquad (\forall i).$$

(23)

The equivalent form of (23) can be expressed as

$$\min_{|X_i(f)|^2, \forall i=1,\ldots,N_t} \sum_{i=1}^{N_t} \int_{\text{BW}} |X_i(f)|^2 \, df,$$

$$\text{s.t. (MI)}_{\text{DMRS}} \simeq \sum_{i=1}^{N_t} T_y \times \int_{\text{BW}} \ln\left\{1 + \frac{|L_i(f)|^2 \times |X_i(f)|^2 \times L_i^2}{T_y \times \left[S_i^{\text{c}}(f) \times |X_i(f)|^2 \times L_i^2 + S_i^{\text{n}}(f)\right]}\right\} df \geq \gamma_{\text{MI}}^{\text{th}},$$

$$\int_{\text{BW}} |X_i(f)|^2 \, df > 0 \qquad (\forall i).$$

(24)

Theorem 4. The solution of the robust optimization problem stated in (24) should satisfy

$$\left|X_i^{\text{robust}}(f)\right|^2 \simeq \max\left[0, \overline{B}_i(f)\left(\overline{A} - \overline{D}_i(f)\right)\right] \qquad (\forall i), \quad (25)$$

where $\overline{B}_i(f)$ and $\overline{D}_i(f)$ can be given by

$$\overline{B}_i(f) = \frac{|L_i(f)|^2 \times L_i^2 / T_y}{2S_i^{\text{c}}(f) \times L_i^2 + |L_i(f)|^2 \times L_i^2 / T_y} \qquad (26)$$

and

$$\overline{D}_i(f) = \frac{S_i^n(f)}{|L_i(f)|^2 \times L_i^2 / T_y}, \qquad (27)$$

respectively, and the constant $\overline{A}$ is chosen now to satisfy

$$\sum_{i=1}^{N_t} T_y \times \int_{\mathrm{BW}} \ln\left\{1 + \frac{|L_i(f)|^2 \times \max\left[0, \overline{B}_i(f)\left(\overline{A} - \overline{D}_i(f)\right)\right] \times L_i^2}{T_y \times \left[S_i^c(f) \times \max\left[0, \overline{B}_i(f)\left(\overline{A} - \overline{D}_i(f)\right)\right] \times L_i^2 + S_i^n(f)\right]}\right\} df \geq \gamma_{\mathrm{MI}}^{\mathrm{th}}.$$

$$(28)$$

From Theorems 3 and 4, it is worth pointing out that the robust transmission waveforms based on LPI-SINR and LPI-MI are formed by performing a water-filling action on the function $\overline{B}_i(f)\left(\overline{A} - \overline{D}_i(f)\right) (\forall i)$.

3. Discussion

One important finding from the above solutions is that in both the LPI-SINR- and LPI-MI-based robust waveform design approaches, the worst case is the lower bound of the target spectrum uncertainty class. Therefore, the optimization of considering both the upper and lower bounds of the uncertainty class is somewhat restrictive [16], [20]. The limitation could be reduced if we remove the upper bound for both the LPI-SINR and LPI-MI cases; that is, the same solutions can also be obtained by employing only the lower bound of the uncertainty class of the target spectrum.

The appropriate waveform design criterion should be chosen based on different tasks in the DMRS, such that the transmission energy could be utilized most efficiently to achieve the best LPI performance. In the robust waveform design criteria, Theorems 3 and 4 are more concerned with the problem of how the LPI-SINR- and LPI-MI-based waveform approaches are affected by the uncertainty of the target spectrum. As indicated in Theorems 3 and 4, the uncertainty of the target spectrum would impact the two criteria in the same way. The same decrease in the target spectrum will lead to the same changes in both criteria. To be specific, a decrease of the target spectrum would result in an increase in the total transmitting energy, which means that the achievable LPI performance of the DMRS would generally degrade. Since the robust waveform design approaches are intended to bound the worst-case LPI performance, we choose the robust waveforms based on the lower bounds of the uncertainty class of the target spectra for both criteria.

IV. Numerical Results

In this section, we provide some numerical results to demonstrate the effectiveness of utilizing the robust

transmission waveforms given in Theorems 3 and 4. For illustrative purposes, Fig. 4 depicts the spatial distribution of the radar nodes in the DMRS with respect to a given known target that is within the radar nodes' detection zones; the purpose of which is to minimize the impact of the topological configuration on the simulation results. The distance between each radar node and the known target is 141.4 km. Throughout this section, G_{ti} and G_{ri} are both set to be 30 dB. We suppose that the power of the additive Gaussian noise is 7.680×10^{-14} W, the duration of the echo T_y is 0.01 s, and $\gamma_{\mathrm{SINR}}^{\mathrm{th}}$ and $\gamma_{\mathrm{MI}}^{\mathrm{th}}$ are set to be 14.43 dB and 5.11 nats, respectively.

The target and interference spectra in the direction of the radar nodes of the DMRS are shown in Figs. 5, 7, 9, and 11. The nominal target spectra are illustrated by the black solid lines. The uncertainty class of each target spectrum is similar to Fig. 3, which is not illustrated for clarity. Figures 6, 8, 10, and 12 depict the LPI-SINR- and LPI-MI-based optimal waveform
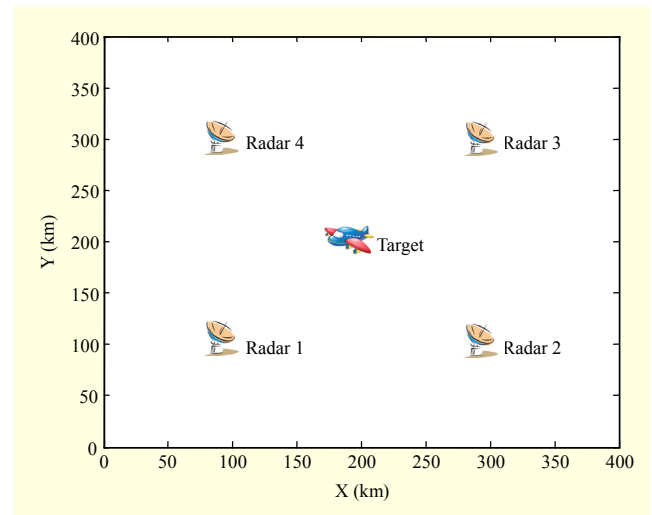

Fig. 4. DMRS and known-target configuration in 2D.
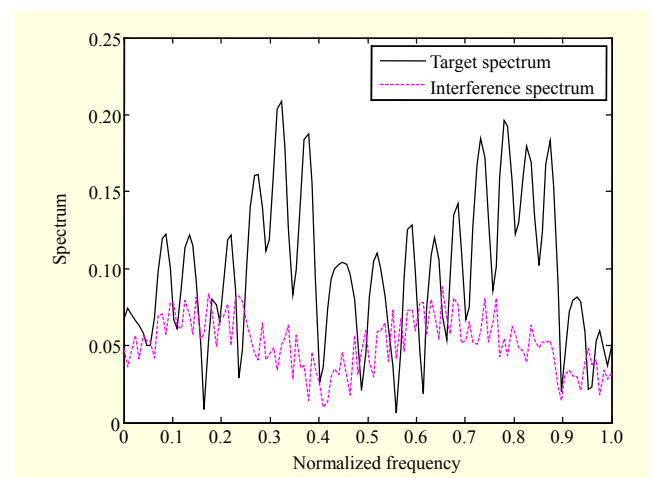

Fig. 5. Target and interference spectra in direction of Radar 1.
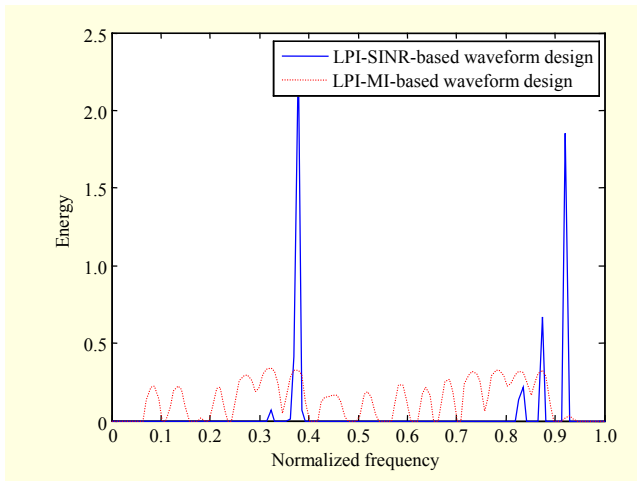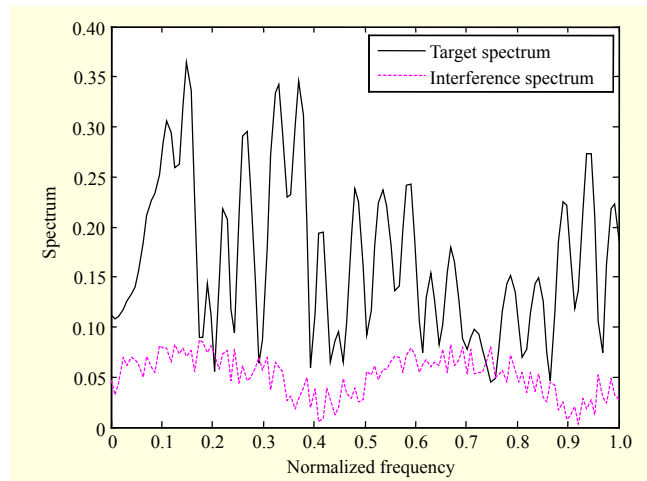
Fig. 6. Optimal waveform design of Radar 1.

Fig. 9. Target and interference spectra in direction of Radar 3.
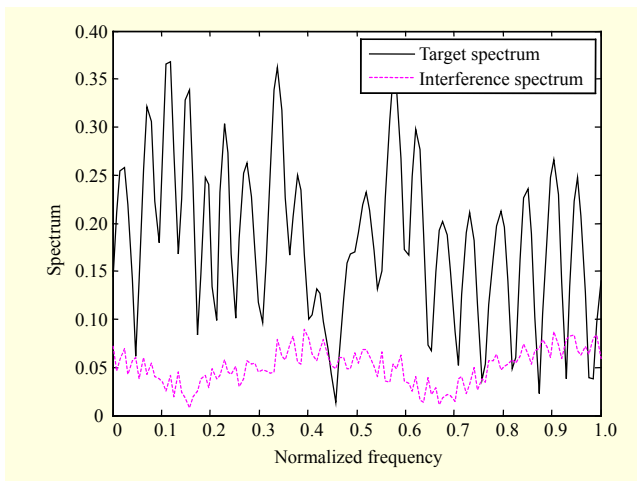

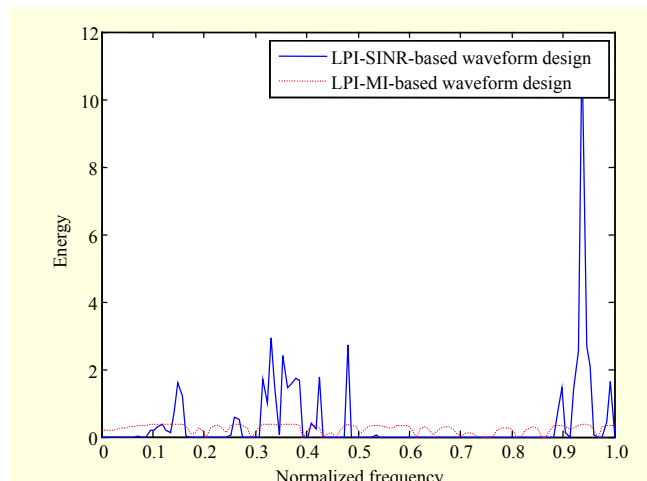Fig. 7. Target and interference spectra in direction of Radar 2.

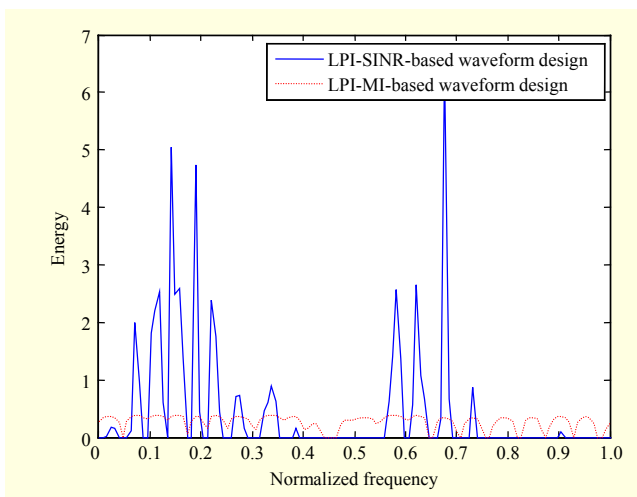Fig. 10. Optimal waveform design of Radar 3.

Fig. 8. Optimal waveform design of Radar 2.

design results, which give insight about the optimal energy allocation for different tasks in the DMRS. The robust waveform results are similar to the optimal waveform results and are not illustrated; in addition, they are only related to the lower bounds of the uncertainty class of the target spectra. For all the radar nodes in the DMRS, it can be seen that the transmission energy allocation is determined by the target spectra relative to the radar nodes and the interference power levels. To be specific, in both the LPI-SINR- and LPI-MI-based waveform design methods, more transmission energy is allocated to those radar nodes that have a larger target spectra and suffer less interference power. To minimize the total transmitting energy for a predetermined threshold of the DMRS's performance, the LPI-SINR-based transmission waveforms are formed by a water-filling action, which only places the minimum energy over the dominant frequency components of the target spectra; that is, the frequency bands with the largest coefficients. In contrast, the LPI-MI-based waveforms tend to distribute the energy over multiple frequency-bands. One reason for this difference is that the calculation
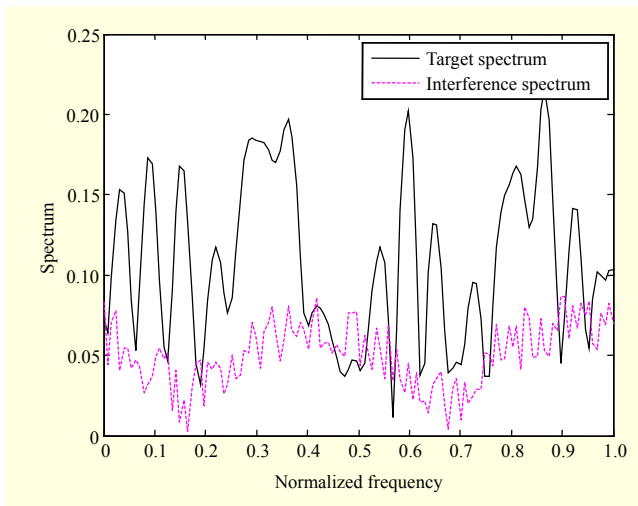
Fig. 11. Target and interference spectra in direction of Radar 4.

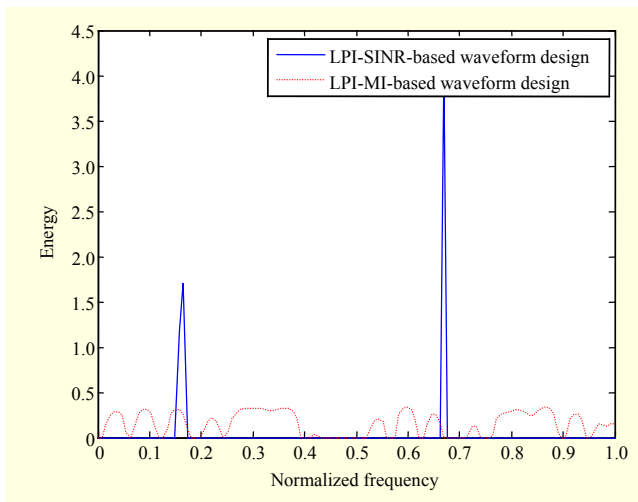Fig. 13. SINR performance curves for robust waveforms.

Fig. 12. Optimal waveform design of Radar 4.

of MI involves log computations, which lowers those terms that are related to the transmission of energy over frequency bands and have large coefficients [16]. Thus, fewer dominant frequency-components would be better. Here, energy is distributed over multiple frequency-bands by performing a water-filling operation. Furthermore, we can observe that both optimized waveforms concentrate their energy in the frequency components where the signal-dependent interference power is potentially the lowest.

The SINR performance curves versus the transmitting energy is depicted in Fig. 13; the results were obtained as a result of 10,000 Monte-Carlo trials. In Fig. 13, the SINR of the DMRS when utilizing the LPI-SINR-based optimal waveforms for a nominal target spectrum [12] ($N_t = 4$), the robust waveforms for LPI-SINR in the worst case ($N_t = 4$), the robust waveforms for LPI-MI in the worst case ($N_t = 4$), the predefined waveforms in the worst case ($N_t = 4$), and the robust
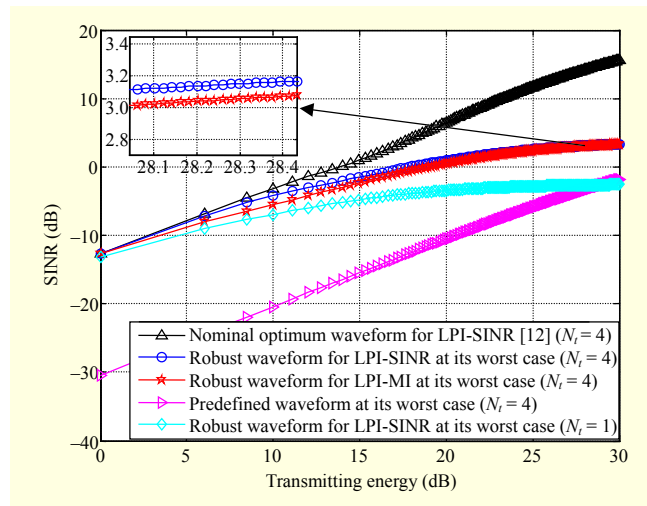
waveforms for LPI-SINR in the worst case ($N_t = 1$) are compared. The results show that the best achievable SINR is obtained when utilizing the optimal waveforms designed for the nominal target spectra, which in turn implies that the DMRS is transmitting the minimum amount of energy for a predefined threshold of SINR. Therefore, the DMRS has the best LPI performance to defend against passive intercept receiver attacks. When the lower envelope in Fig. 3 is the worst case in the uncertainty class, the robust waveform design approaches are employed. It is not surprising that the robust waveforms transmit more energy than the nominal optimal waveforms for a predetermined threshold of target detection performance due to the fact that the robust waveform design approaches have less prior knowledge about the target spectra. However, if the robust waveforms are used, then the achievable LPI performance would not be worse than this bound; thus, the LPI performance will be guaranteed. It can be concluded that the robust transmission waveform for LPI-SINR is optimum for the worst-case target spectrum in the uncertainty class.

Predefined waveforms are those that allocate transmitting energy uniformly over the whole of a frequency band with no prior knowledge of the known target, and which have the worst-case LPI performance. It is obvious that the worst-case LPI performance of the robust waveforms can be significantly enhanced over the worst-case LPI performance of the predefined waveforms. This further confirms the effectiveness of exploiting the robust waveforms. Moreover, to compare the two robust waveforms obtained under different criteria, a red pentagram line is plotted in Fig. 13, which can be obtained by employing the robust waveforms for LPI-MI when the true target spectra are the lower bounds of the uncertainty classes of the target spectra. Obviously, the robust waveforms based on LPI-MI exhibit a much inferior LPI performance than the LPI-
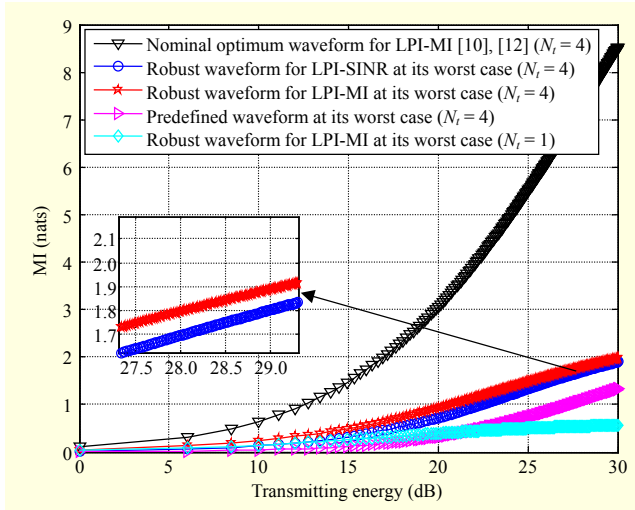
Fig. 14. MI performance curves for robust waveforms.

SINR-based case. This is because of the misapplication of the robust waveforms, which gives insight into the inherent difference between the two robust waveform design criteria [16]. In addition, we can see that the available SINR of the LPI-SINR-based robust waveforms in the worst case ($N_t = 4$) is much larger than that in the case $N_t = 1$. This is because a DMRS can provide great spatial diversity in terms of the achievable target detection performance, which in turn strengthens the LPI benefits of using a DMRS.

Similar to Fig. 13, we show the MI performance curves versus the transmitting energy in Fig. 14, which corresponds to the MI of the DMRS when utilizing the LPI-MI-based optimal waveforms for the nominal target spectrum [10], [12] ($N_t = 4$), the robust waveforms for LPI-MI in the worst case ($N_t = 4$), the robust waveforms for LPI-SINR in the worst case ($N_t = 4$), the predefined waveforms in the worst case ($N_t = 4$), and the robust waveforms for LPI-MI in the worst case ($N_t = 1$), respectively. It is worth pointing out that for MI, the worst-case performance can be obtained when the true target spectra are the lower envelopes as illustrated in Fig. 3. Additionally, we also plot a blue round line in Fig. 14, which can be achieved by utilizing the robust waveforms for LPI-SINR when the true target spectra are the lower envelopes of the uncertainty classes of the target spectra. One can observe from Fig. 14 the benefits of utilizing the robust waveforms for LPI-MI. However, the worst-case performance enhancement of employing LPI-MI-based robust waveforms is less remarkable than that of employing the LPI-SINR-based robust waveform design criterion, which is due to the fact that the calculation of MI involves the logarithm function and scales the effect down. When the target spectrum lies in the uncertainty class, the achievable LPI performance will be always as good as or better than the robust waveforms in the worst case, which is not

surprising since the robust waveform effectively bounds the worst possible LPI performance over the entire uncertainty class. Besides, it should be noted that the presented robust waveform design approaches based on LPI-SINR and LPI-MI are significantly simple to implement and can achieve better LPI performance in a DMRS. In various cases, the effectiveness and benefits of exploiting robust waveforms would be more or less the same [20]. Thus, it is worth pointing out that using a robust transmission waveform design optimizes the worst-case LPI performance, and it is a well-accepted engineering approach.

V. Conclusion

In this paper, the approaches of task-dependent robust transmission waveform design for a DMRS based on LPI are presented, where the uncertainty of the target spectrum is considered. A band model is utilized by assuming that the target spectrum lies in an uncertainty class with known upper and lower bounds. With the limited knowledge of the target spectrum, robust waveform design methods are developed for the DMRS under LPI-SINR and LPI-MI criteria. Numerical results demonstrate that the proposed approaches are effective in enhancing the LPI performance of the DMRS in the worst possible scenario. For our future research, we intend to focus on other optimization criteria to enhance the robust LPI performance of a DMRS.

References

[1] E.P. Phillip, "*Detecting and Classifying Low Probability of Intercept Radar*," Boston, USA: Artech House, 2009, pp. 342–352.

[2] E. Fishler et al., "Spatial Diversity in Radars–Models and Detection Performance," *IEEE Trans. Signal Process.*, vol. 54, no. 3, Mar. 2006, pp. 823–838.

[3] C.G Shi et al., "LPI Optimization Framework for Target Tracking in Radar Network Architectures Using Information-Theoretic Criteria," *Int. J. Antennas Propag.*, vol. 2014, July 2014, pp. 1–10.

[4] B. Friedlander, "Waveform Design for MIMO Radars," *IEEE Trans. Aerosp. Electron. Syst.*, vol. 43, no. 3, July 2007, pp. 1227–1238.

[5] P. Stoica, J. Li, and Y. Xie, "On Probing Signal Design for MIMO Radar," *IEEE Trans. Signal Process.*, vol. 55, no. 8, Aug. 2007, pp. 4151–4161.

[6] M.R. Bell, "Information Theory and Radar Waveform Design," *IEEE Trans. Inf. Theory*, vol. 39, no. 5, Sept. 1993, pp. 1578–1597.

[7] Y. Yang and R.S. Blum, "MIMO Radar Waveform Design Based on Mutual Information and Minimum Mean-Square Error

Estimation," *IEEE Trans. Aerosp. Electron. Syst.*, vol. 43, no. 1, Jan. 2007, pp. 330–343.

[8] M.M. Naghsh et al., "Unified Optimization Framework for Multi-static Radar Code Design Using Information-Theoretic Criteria," *IEEE Trans. Signal Process.*, vol. 61, no. 21, Nov. 2013, pp. 5401–5416.

[9] Y.F. Chen et al., "Adaptive Distributed MIMO Radar Waveform Optimization Based on Mutual Information," *IEEE Trans. Aerosp. Electron. Syst.*, vol. 49, no. 2, Apr. 2013, pp. 1374–1385.

[10] L. Xu and Q.L. Liang, "Waveform Design and Optimization in Radar Sensor Network," *IEEE Conf. Global Telecommun.*, Miami, FL, USA, Dec. 6–10, 2010, pp. 1–5.

[11] B. Tang, J. Tang, and Y.N. Peng, "MIMO Radar Waveform Design in Colored Noise Based on Information Theory," *IEEE Trans. Signal Process.*, vol. 58, no. 9, Sept. 2010, pp. 4684–4697.

[12] R.A. Romero, J. Bae, and N.A. Goodman, "Theory and Application of SNR and Mutual Information Matched Illumination Waveforms," *IEEE Trans. Aerosp. Electron. Syst.*, vol. 47, no. 2, Apr. 2011, pp. 912–927.

[13] P.M. Woodward, "Theory of Radar Information," *Trans. IRE Professional Group Inf. Theory*, vol. 1, no. 1, Feb. 1953, pp. 108–113.

[14] P.M. Woodward, "Information Theory and the Design of Radar Receivers," *Proc. IRE*, vol. 39, no. 12, Dec. 1951, pp. 1521–1524.

[15] S.A. Kassam and H.V. Poor, "Robust Techniques for Signal Processing: A Survey," *Proc. IEEE*, vol. 73, no. 3, Mar. 1985, pp. 433–481.

[16] Y. Yang and R.S. Blum, "Minimax Robust MIMO Radar Waveform Design," *IEEE J. Sel. Topics Signal Process.*, vol. 1, no. 1, June 2007, pp. 147–155.

[17] B. Jiu et al., "Minimax Robust Transmission Waveform and Receiving Filter Design for Extended Target Detection with Imprecise Prior Knowledge," *Signal Process.*, vol. 92, no. 1, Jan. 2012, pp. 210–218.

[18] Y.Q. Zhao, C.L. Yu, and H.P. Yin, "Research into the Anti-Common-Frequency Interference Technology Based on Code-Agility," *Shipboard Electron. Countermeasure*, vol. 36, no. 1, Jan. 2013, pp. 14–19.

[19] C.G. Shi, J.J. Zhou, and F. Wang, "Low Probability of Intercept Optimization for Radar Network Based on Mutual Information," *IEEE China Summit Int. Conf. Signal Inf. Process.*, Xi'an, China, July 9–13, 2014, pp. 683–687.

[20] L.L. Wang et al., "Minimax Robust Jamming Techniques Based on Signal-to-Interference-Plus-Noise Ratio and Mutual Information Criteria," *IET Commun.*, vol. 8, no. 10, July 2014, pp. 1859–1867.

Chenguang Shi received his BS degree in electronic information science and technology from the College of Electronic and Information Engineering, Nanjing University of Aeronautics and Astronautics (NUAA), China, in 2012. He is currently working toward his PhD degree at NUAA at the Key Laboratory of Radar Imaging and Microwave Photonics, Ministry of Education. His main research interests include target tracking, parameter estimation, and radar signal processing.

Fei Wang received his MS and PhD degrees in communications and information systems from the College of Communications Engineering, Jilin University, Changchun, China, in 2003 and 2006 respectively. He is currently an associate professor at Nanjing University of Aeronautics and Astronautics, China. His main research interests include aircraft radio frequency stealth, radar signal processing, and array signal processing.

Mathini Sellathurai received her technical licentiate degree in signal processing and communications from the Royal Institute of Technology, Stockholm, Sweden, in 1997 and her PhD degree in signal processing and communications systems from McMaster University, Hamilton, Canada, in 2001. She is currently an associate professor at Heriot-Watt University, Edinburgh, UK. Her current research interests include adaptive and statistical signal processing; space–time and MIMO communications theory; network coding; information theory; and cognitive radio. She was the recipient of the Natural Sciences and Engineering Research Council of Canada's Doctoral Award for her PhD dissertation and a co-recipient of the IEEE Communication Society 2005 Fred W. Ellersick Best Paper Award. She is currently serving as an associate editor for IEEE Transactions on Signal Processing.

Jianjiang Zhou received his MS and PhD degrees in radar signal processing from Nanjing University of Aeronautics and Astronautics (NUAA), China, in 1988 and 2001, respectively. He is currently both a professor and a director of the Key Laboratory of Radar Imaging and Microwave Photonics, Ministry of Education, NUAA. His main research interests include aircraft radio frequency stealth, radar signal processing, and array signal processing.

Huan Zhang received her BS degree in information engineering from Nanjing University of Aeronautics and Astronautics (NUAA), China, in 2013. She is currently working toward her MS degree in signal processing at NUAA at the Key Laboratory of Radar Imaging and Microwave Photonics, Ministry of Education. Her main research interests include target tracking, radar waveform optimization, and signal processing.